– Supplementary Information –

Charging C_{60} Islands with the AFM Tip

Brice Hoff, Claude R. Henry, and Clemens Barth*

CNRS, Aix-Marseille University, CINaM UMR 7325, Campus de Luminy, Case 913, 13288 Marseille Cedex 09, France

E-mail: barth@cinam.univ-mrs.fr

Abstract

This Supplementary Information of the main article *Charging C_{60} Islands with the AFM Tip* comments the sample preparation, experimental methods, and supporting experiments, which are linked with the main article.

1 Sample preparation

Millimeter thick NaCl single crystals of highest purity (size: $4 \times 4 \times 10$ mm^2) are outgased by annealing at ~ 200°C in an oven, which is located inside the UHV chamber[1]. After cooling of the crystals and the sample holder, a clean (001) surface is obtained by *in-situ* cleavage of a crystal along the (001) plane at room temperature. The crystals are then annealed again in UHV at around ~ 200°C for a few hours to put the crystals into their equilibrium charge state, as described in Ref. Barth07. After the surface preparation, a NaCl(001) surface exhibits one mono-layer (ML) high steps with a typical density of 10^8 to 10^9 steps/cm^2 and atomically flat terraces with a width of up to a few hundreds of nanometer. One ML is defined here as one NaCl crystallographic plane, which height h_{ML} is half the unit cell ($a_{\mathrm{NaCl}} = 0.564$ nm[3]) in the [001] direction, $h_{\mathrm{ML}} = a_{\mathrm{NaCl}}/2 = 0.282$ nm. The C_{60} molecules (99.9% purity, Alfa Aesar, Karlsruhe, Germany) are evaporated at 330°C from a Knudsen cell (TCE-BCS 3 cell evaporator, Kentax GmbH, Seelze, Germany) onto the substrate kept at room temperature, with a deposition rate of 0.3 ML/min. The nominal thickness of evaporated C_{60} for all experiments shown in this work was around 0.5 ML. Before the deposition, the molecules are purified during an annealing in the Knudsen cell at similar temperatures.

*To whom correspondence should be addressed

2 AFM methods

Noncontact AFM (nc-AFM) experiments are conducted with a room temperature AFM/STM system (Scienta Omicron GmbH, Taunusstein, Germany) in a UHV chamber maintaining a base pressure in the low 10^{-10} mbar range. Conducting silicon cantilevers with a resonance frequency between 280 and 320 kHz (Nanosensors, type PPP-QNCHR, p-Si, 0.015 Ω cm - NanoWorld AG, Neuchatel, Switzerland) are used, whereas the tip used for the experiments shown here had a resonance frequency of 278.4 Hz. The instrument is operated in the frequency modulation mode with an oscillation amplitude of some nanometers where frequency demodulation is accomplished by an EasyPLL demodulator (NanoSurf, Liestal, Switzerland).

We use frequency modulated Kelvin probe force microscopy (FM-KPFM)[4,5] and electrostatic force microscopy (FM-EFM)[6,7] where a DC (U_{dc}) and AC voltage ($U_{\mathrm{ac}} = 1.5$ V) with frequency $f_{\mathrm{ac}} = 475$ Hz are applied at the sample (tip is grounded) during the nc-AFM topography imaging mode (constant $\triangle f$ mode). In this case the capacitive force, F_{C}, between tip and surface is given by

$$F_{\mathrm{C}} = \frac{1}{2}\frac{\partial C}{\partial z}\left(U_{\mathrm{DC}} + U_{\mathrm{AC}}\sin\left(2\,\pi\,f_{\mathrm{AC}}\,t\right) - U\right)^2 \qquad (1)$$

where $\partial C/\partial z$ is the capacitance gradient between tip and sample surface. The potential difference U is the apparent contact potential difference (CPD) between

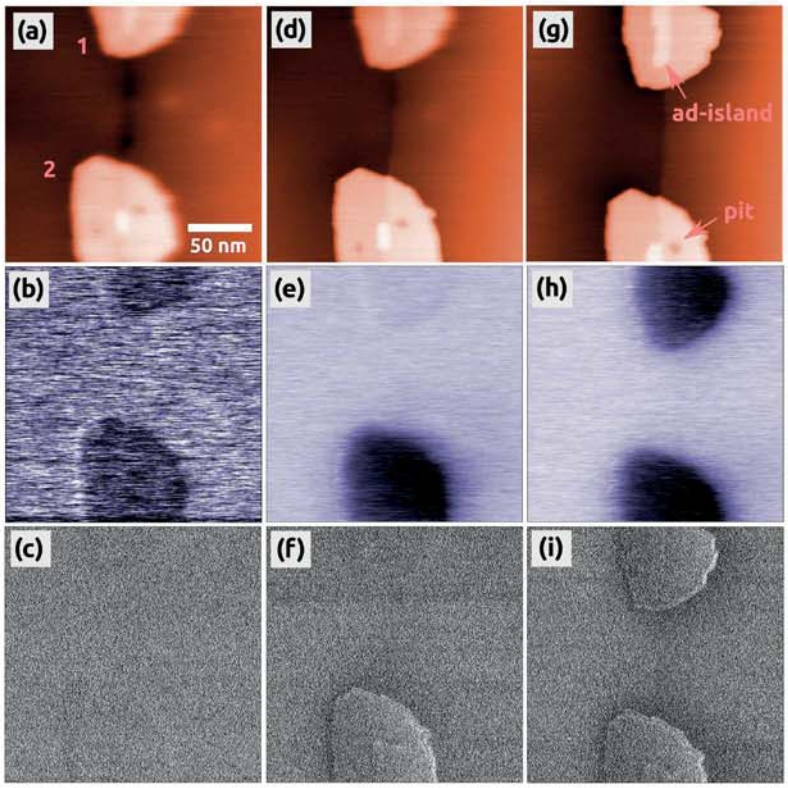

Fig. S1: Three EFM measurements of the two C_{60} islands, which were intentionally charged as documented in Fig. 2 of the main article. A column of images corresponds to one EFM measurement. The images (a), (d) and (g) represent the topography, images (b), (e) and (h) the EFM signal and images (c), (f) and (i) the damping signal. The EFM images (b, e and h) are shown in the main article in Fig. 2c, g and h. From the last damping image (i) the following values for the damping (Γ) were extracted: $\Gamma_{\mathrm{NaCl}} = 1.033$, $\Gamma_{\mathrm{Island}} = 1.027$ (averaged over the whole island), $\Gamma_{\mathrm{Left\ edge}} = 0.99$ (min) and $\Gamma_{\mathrm{Right\ edge}} = 1.10$ a.u. (max). Size: 200×200 nm^2, speed: 0.5 Hz, $\triangle f = -11.8$ (a) to (c), -13.8 (d) to (f) and -13.8 (g) to (i), EFM bias voltage: $+2.0$ V.

the sample holder carrying the NaCl crystal and the tip[8]. The CPD is therefore influenced by the dielectric properties of NaCl and by charges inside the NaCl sample and in particular on the NaCl(001) surface[2,5]. Equation (1) can be expanded such that three force parts are obtained:

$$F_{\mathrm{C}} = \frac{1}{2}\frac{\partial C}{\partial z}\left((U_{\mathrm{DC}} - U)^2 + \frac{1}{2}U_{\mathrm{AC}}^2\right) \quad (2)$$

$$+ \frac{\partial C}{\partial z}(U_{\mathrm{DC}} - U)\,U_{\mathrm{AC}}\sin(2\,\pi\,f_{\mathrm{AC}}\,t) \quad (3)$$

$$- \frac{1}{4}\frac{\partial C}{\partial z}U_{\mathrm{AC}}^2\cos(2\cdot 2\,\pi\,f_{\mathrm{AC}}\,t) \quad (4)$$

Equation (2) describes the static part and in particular the parabolic dependence of the capacitive force F_{C} on the applied bias voltage U_{DC}. The third part (Eq. (4)) is the *second harmonic* and oscillates at the frequency $2\,f_{\mathrm{ac}}$. The second part of the equation (Eq. (3)) is the *first harmonic* including the important sum of voltages, $U_{\mathrm{DC}} - U$, which contains the contribution of charges on and below the NaCl(001) surface.

During a KPFM measurement, the bias voltage U_{DC} is varied by a feedback loop such that the amplitude of the first harmonic (Eq. (3)) is zero. This is always the case when $U_{\mathrm{DC},0} = U$ where the electrostatic tip-surface interaction is minimized by the DC voltage, as it can be easily seen in Eq. (1). In our Kelvin set-up, the condition $U_{\mathrm{DC},0} = U$ is reached at almost each tip-position during the normal topography imaging mode, so that a second, so-called *Kelvin image* is simultaneously recorded directly representing $U_{\mathrm{DC},0} = U$ (*Kelvin*

voltage). In our set-up, a bright Kelvin contrast corresponds to more positive Kelvin voltages and *vice-versa*.

In the frequency modulated EFM mode, the Kelvin feedback loop is deactivated and a constant DC voltage U_{dc} is applied. The amplitude of the first harmonic (Eq. (3)) is then recorded in a separate so-called *EFM image*, as explained in Ref. Terris89 and Schierle97a. Because the sum of voltages, $U_{\mathrm{DC}} - U$, is contained in the first harmonic, EFM images represent the contribution of charges on and below the NaCl(001) surface.

All images are acquired with the Omicron SCALA system and processed with the open-source software Gwyddion [9]. Topography, EFM and Kelvin images shown in this work were always recorded in the forward scanning direction if not mentioned otherwise.

3 Damping signal of charged C_{60} islands

In Fig. S1, three EFM measurements are shown, with each column of images obtained within one EFM measurement. The images represent the topography (a, d, g), EFM (b, e, h) and damping signal (c, f, i) before, during and after the the charging of the two islands. The EFM images (b, e, h) are discussed in the main article in Fig. 2c, g and h. All images were obtained with the same tip and same scanning parameters.

As it can be clearly seen by a comparison of the topography images in Fig. S1a, d and g, the morphology of the islands did not change on the nanometer scale after the first (d) and second charging (g) of island 2 and 1, respectively: for instance, the same shape of the islands but also same features like the two pits on island 2 as well as the ad-islands, which can be found on top and in the middle of the islands, can be found in all images. Although no molecular resolution was obtained, we anticipate that there were also no significant changes in the molecular structure of the islands after the charging.

The island contrast in the topography in Fig. S1a is a bit blurred in comparison to the island contrast in Fig. S1g. The same blurred contrast can be found in image Fig. S1d at the top island 1. In other words, an island contrast got always sharp after the charging of an island. The reason for this is that in Fig. S1a the two islands were imaged under the condition of a strong electrostatic field between tip and island (see discussion in the main article). The electrostatic tip-surface interaction obviously contributed to a large extend such that the van der Waals contribution, which is responsible for the topography contrast, was relatively small since the image was obtained in the constant $\triangle f$ mode, with $\triangle f = \triangle f_{\text{van der Waals}} + \triangle f_{\mathrm{el}} = \triangle f_{\text{pre-set}}$=const. ($\triangle f_{\text{pre-set}}$: pre-set value of the detuning, chosen by the user). After the charging of an island, the electrostatic force between the charged island and the tip was reduced, which resulted into a larger contribution of van der Waals forces - the tip moved closer to surface and the island contrast got sharper.

Before the charging, both islands did not exhibit a preferred damping contrast, as it can be seen in Fig. S1c. However, as soon as an island got charged the damping (Γ) slightly changed: a preferred contrast at the charged island 1 in Fig. S1f is characterized by dark and white island edges, whereas the interior of the island has almost the same contrast as before, being comparable to the contrast of the NaCl(001) regions (averaged Γ value on the islands is by 0.5 % smaller in comparison to the value obtained on NaCl(001)). The uncharged island on the top exhibits no contrast, which, however, changed after the island had also been charged by the AFM tip (see Fig. S1i). The change of contrast at the edges is very small and measures roughly 4 to 6 %. After the EFM images had been obtained on the two charged islands, we switched to the KPFM mode. In the top row of Fig. S2, a KPFM measurement is shown, with images representing the topography (a), Kelvin voltage (b) and damping signal (c). We could detect a faint damping contrast at the two charged islands, with small differences with respect to the NaCl(001) terraces. The damping is now almost homogeneously distributed all over the islands, with changes of about 1 % with respect to NaCl(001).

We strongly anticipate that the preferred contrast at the edges of the islands in the EFM images (Fig. S1) is a result of the scanning and tip-surface distance as follows: firstly, it is clear that the dark/white contrast at the edges is a result of the scanning direction, which was directed from the right to the left (backward scanning direction) in all damping images. The contrast should be reversed in the image of the forward scanning direction, however, unfortunately we did not obtained such an image. Secondly, because of the differences in the topography contrast at the islands 1 and 2 in Fig. S1f, the tip was closer to the charged island 2 in comparison to the uncharged island 1. This could be the reason that at island 2 a clear change of the damping could be measured, whereas it was simply too small in the case of the uncharged island 1 due to the larger tip-island distance. And indeed, in Fig. S2 the two successive KPFM measurements, (d) to (f) and (g) to (i), exemplify the influence of the tip-surface distance on the damping: in the first measurement (d-f), the *uncharged* C_{60} islands in image (e) exhibit only a faint contrast at a pre-set value of $\triangle f = -11.7$ Hz. In the following measurement (g-i), the pre-set value of the detuning was decreased onto $\triangle f = -21.5$ Hz such that the tip approached closer to

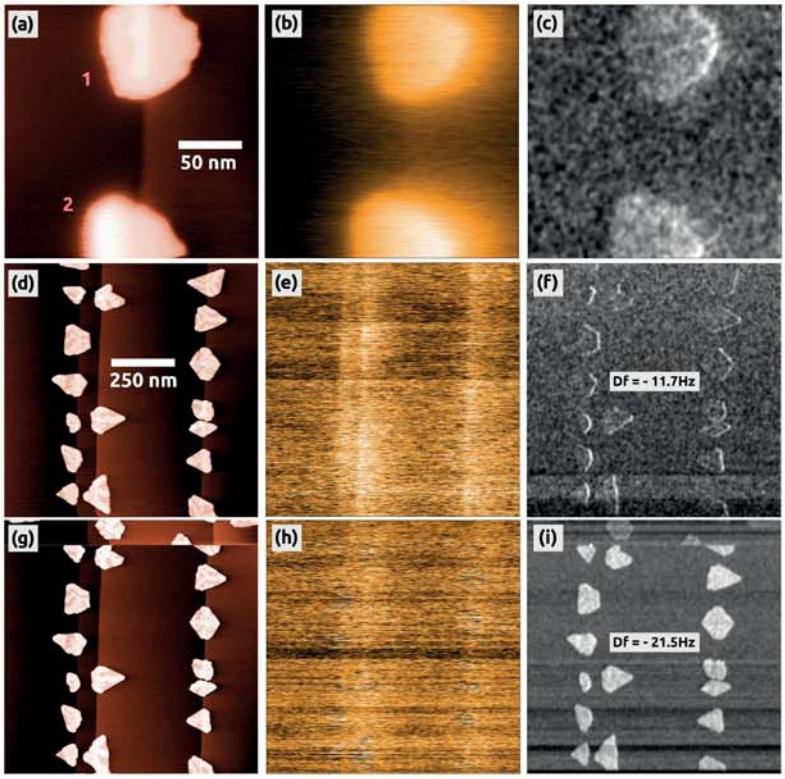

Fig. S2: a)-c) A KPFM measurement of the two C_{60} islands, which were intentionally charged as documented in Fig. 2 of the main article. The image (a) shows the topography whereas images (b) and (c) show the Kelvin voltage and damping signal. The damping image (c) was obtained after an application of a Gauss filter (10 pixel Gauss filter, processed with Gwyddion[9]). Damping contrast Γ: $\Gamma_{\mathrm{NaCl}} = 0.962$, $\Gamma_{\mathrm{Island}} = 0.973$ a.u. (averaged over the whole islands). Image size: 200×200 nm^2, speed: 0.5 Hz, $\triangle f = -7.4$ Hz. d)-i) KPFM measurements of uncharged C_{60} islands on NaCl(001). Shown are the topography (d, g), Kelvin voltage (e, h) and damping signal (f, i). A row of images corresponds to one KPFM measurement. Damping contrast Γ: (f) $\Gamma_{\mathrm{NaCl}} = 0.929$, $\Gamma_{\mathrm{Island}} = 0.93$ a. u. (i) $\Gamma_{\mathrm{NaCl}} = 0.984$ (min: 0.96, max: 1.0), $\Gamma_{\mathrm{Island}} = 1.043$ a. u. (averaged). Image size: 1000×1000 nm^2, speed: 0.5 Hz, $\triangle f = -11.7$ (d) to (f) and -21.5 Hz (g) to (i).

the surface. The result is that the islands appear in a clear white damping contrast, which corresponds to a 6 % change of the damping with respect to NaCl(001).

Considering the last two aspects, we exclude the phenomena that a charge inside the C_{60} islands produces a preferred damping contrast similar to the one shown in Fig. S1f and i. With respect to the observed damping contrast as such the detailed mechanism remains unknown so far. We can only state that we always observed a brighter damping contrast (higher damping value) at the C_{60} islands with respect to NaCl(001), which means that more energy of the cantilever oscillation got lost at the C_{60} islands. On the one hand one can speculate that the damping contrast is a result of an energy dissipation into the islands due to the softness of the islands. On the other hand it is well known that energy can be also dissipated into the tip as discussed in, e.g., Refs.[10–12]. The tip's influence on the damping can be easily understood when carefully analyzing the damping image in Fig. S2f and in particular in Fig. S2i: at several places the damping contrast of NaCl(001) changed by a few percent within a single scanning line, which resulted into parallel bands of high (bright) and low damping values (dark). Such changes can be unambiguously assigned to changes at the tip.

To study damping phenomena at C_{60} islands, more systematic experiments need to be done, probably in conjunction with theory.

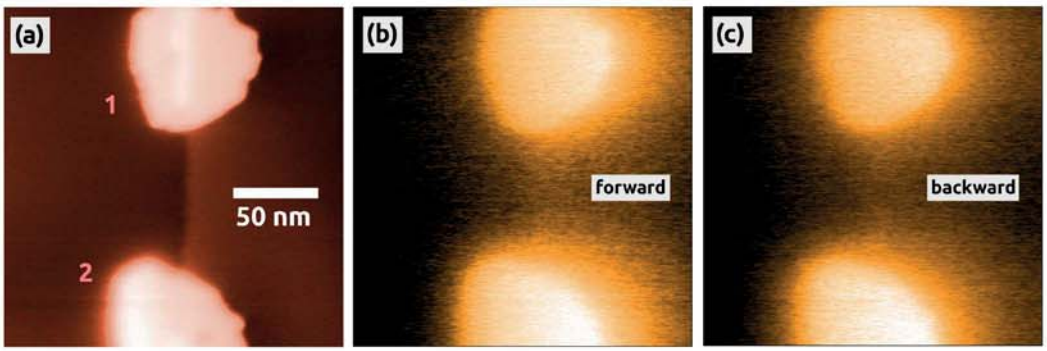

Fig. S3: A KPFM measurement of the two C_{60} islands, which were intentionally charged as documented in Fig. 2 of the main article. The measurement was obtained after the KPFM measurement shown in Fig. S2a to c. Image (a) shows the topography whereas images (b) and (c) show the Kelvin voltage in forward and backward scanning direction. The Kelvin image (b) is the same image as the one in Fig. 3a of the main article. Size: 200×200 nm^2, speed: 0.5 Hz, $\triangle f = -7.4$ Hz.

4 Kelvin contrast of charged C_{60} islands

An important characteristic of the Kelvin images shown in Fig. 3 and 4 of the main article is that the two charged C_{60} islands appear in a bright Kelvin contrast, which gradually increases from the left to the right side of the island. This particular contrast phenomena did not depend on the scanning as shown in Fig. S3, which shows apart from the topography image (Fig. S3a), the two simultaneously obtained Kelvin images recorded in the forward (Fig. S3b) and backward scanning direction (Fig. S3c): both Kelvin images exhibit same contrast details so that a potential artifact, e.g., depending on the two different scanning directions can be clearly excluded.

The reason for the gradual increase of the Kelvin contrast remains unknown. We speculate that this contrast phenomena was probably due a tip effect: when the tip was located above the left part of the island on the lower terrace, the tip had a larger interaction volume with both NaCl(001) terraces than in the case when the tip was located above the right part of the island (higher NaCl(001) terrace). This might result into a reduction of the Kelvin voltage on the left side because the tip obtained more signal from the NaCl regions. When the tip scanned the island from, e.g., the left to the right (forward scanning direction), the interaction volume with NaCl decreased gradually resulting into a smooth increase of the Kelvin voltage. The same applies during scanning an island from the right to the left side (backward scanning direction). Apart from this model, there also is the possibility that the contrast was due to an asymmetric shape of the tip. To explain the contrast and verify both models calculations need to be done in future.

References

(1) Barth, C.; Claeys, C.; Henry, C. R. *Rev. Sci. Instr.* **2005**, *76*, 083907.
(2) Barth, C.; Henry, C. R. *Phys. Rev. Lett.* **2007**, *98*, 136804.
(3) Prada, S.; Martinez, U.; Pacchioni, G. *Phys. Rev. B* **2008**, *78*, 235423.
(4) Kitamura, S.; Iwatsuki, M. *Appl. Phys. Lett.* **1998**, *72*, 3154–3156.
(5) Barth, C.; Henry, C. R. *Nanotechnology* **2006**, *17*, S155–S161.
(6) Terris, B. D.; Stern, J. E.; Rugar, D.; Mamin, H. J. *Phys. Rev. Lett.* **1989**, *63*, 2669–2672.
(7) Nyffenegger, R. M.; Penner, R. M.; Schierle, R. *Appl. Phys. Lett.* **1997**, *71*, 1878–1880.
(8) Ogawa, S.; Ichikawa, S. *Phys. Rev. B* **1995**, *51*, 17231–17234.
(9) www.Gwyddion.net, 2014.
(10) Sasaki, N.; Tsukada, M. *Jpn. J. Appl. Phys., Part 2* **2000**, *39*, L1334–L1337.
(11) Kawai, S.; Canova, F. F.; Glatzel, T.; Foster, A. S.; Meyer, E. *Phys. Rev. B* **2011**, *84*, 115415.
(12) Canova, F. F.; Kawai, S.; de Capitani, C.; Glatzel, T.; Such, B.; Foster, A. S.; Meyer, E. *Phys. Rev. Lett.* **2013**, *110*, 203203.